Ocean Systems Engineering, *Vol. 7, No. 3 (2017) 299-318*
DOI: https:// doi.org/10.12989/ose.2017.7.3.299

Towards development of a reliable fully-Lagrangian MPS-based FSI solver for simulation of 2D hydroelastic slamming

Abbas Khayyer*, Hitoshi Gotoh, Hosein Falahaty,
Yuma Shimizu and Yusuke Nishijima

Department of Civil and Earth Resources Engineering, Kyoto University,
Katsura Campus, Nishikyo-ku, Kyoto 615-8540, Japan

(Received July 21, 2017, Revised August 15, 2017, Accepted August 17, 2017)

Abstract. The paper aims at illustrating several key issues and ongoing efforts for development of a reliable fully-Lagrangian particle-based solver for simulation of hydroelastic slamming. Fluid model is founded on the solution of Navier-Stokes along with continuity equations via an enhanced version of a projection-based particle method, namely, Moving Particle Semi-implicit (MPS) method. The fluid model is carefully coupled with a structure model on the basis of conservation of linear and angular momenta for an elastic solid. The developed coupled FSI (Fluid-Structure Interaction) solver is applied to simulations of high velocity impact of an elastic aluminum wedge and hydroelastic slammings of marine panels. Validations are made both qualitatively and quantitatively in terms of reproduced pressure as well as structure deformation. Several remaining challenges as well as important key issues are highlighted. At last, a recently developed multi-scale MPS method is incorporated in the developed FSI solver towards enhancement of its adaptivity.

Keywords: hydroelasticity; slamming; fluid structure interaction; moving particle semi-implicit

1. Introduction

Hydrodynamic slamming loads are of substantial importance to maritime engineering (e.g. design of ships, offshore platforms, buoys and etc.). Thus, several experimental, analytical and numerical studies have been dedicated to the evaluation of hydrodynamic slamming effects on rigid structures (e.g., Zhao and Faltinsen 1993, Faltinsen 2002, De Backer *et al*. 2009, Aly *et al*. 2011, Lind *et al*. 2015, Wang *et al*. 2015, Zhao *et al*. 2015). However, in cases of violent slamming loads, the local effects of structural deformations would be of significant contribution to the hydrodynamics and vice versa and examples include local slamming effects on ships hulls or platforms in storm conditions. Moreover, in line with advancements of marine design in application of light weight deformable materials (e.g., light weight composites in high speed crafts), the effect of structural deformability in marine systems has become more important. Therefore, the complex mutual relationships in between hydrodynamics and structural responses, the so-called hydroelasticity effects, in slamming phenomena is of great significance.

The effect of hydroelasticity has been the target of many analytical, experimental or numerical

*Corresponding author, Associate Professor, E-mail: khayyer@particle.kuciv.kyoto-u.ac.jp

http://www.techno-press.org/?journal=ose&subpage=7 ISSN: 2093-6702 (Print), 2093-677X (Online)

studies. In this regard, Faltinsen (1999) carried out a comprehensive study on the hydrodynamics-structure system of wedge-shaped hull water entry based on coupling between generalized Wagner's theory (Wagner 1932) and orthotropic plate theory in line with conduction of full-scale experiments. Similarly, Scolan (2004) investigated the hydroelastic effects by coupling a Wagner's theory to a linear model of elasticity for thin shells. Tay and Wang (2012) presented a study on reducing the hydroelastic response of very large floating structures (VLFS) by altering their plan shapes. Also, modeling of hydroelasticity has been carried out in the frame of coupling between analytical theories to mesh-based structural solvers for further verification of experimental results (e.g., Peseux *et al.* 2005, Stenius *et al*. 2013, Liu *et al*. 2015, Wang *et al*. 2015).

As for numerical studies, so far the hydroelasticity effects have been studied by a variety of coupling methods founded on mesh-based solvers such as explicit Arbitrary Lagrange Euler-Finite Element Methods, ALE-FEM (e.g., Aquelet and Souli 2003, Das and Batra 2011, Sun and Faltinsen 2006). However, with respect to intrinsic characteristics of hydroelastic phenomena i.e., free surface flows accompanied by large deformations, Lagrangian meshfree methods, namely, particle methods, e.g., Smoothed Particle Hydrodynamics (SPH; Lucy 1977, Gingold and Monaghan 1977) or Moving Particle Semi-implicit (MPS; Koshizuka and Oka 1996), possess distinct potential advantages. Particle methods have been coupled with either semi-analytical or mesh-based methods for simulation of FSI problems, e.g., coupled MPS-modal superposition method (e.g., Sun *et al*. 2015), coupled SPH-FEM (e.g., Campbell and Patel 2010, Fourey *et al*. 2010, Panciroli *et al*. 2012, Yang *et al.* 2012) or coupled MPS-FEM (e.g., Zhang *et al*. 2016). In this regard, a crucial issue corresponds to the consistency of the coupling schemes in between meshfree fluid and mesh-based structure models to achieve an accurate imposition of fluid-structure interface boundary conditions (e.g., stress/velocity continuity).

A number of studies have targeted hydroelastic slamming using particle-based methods in an integrated fully-Lagrangian meshfree framework that can potentially lead to an accurate and consistent imposition of fluid-structure interface boundary conditions. In a pioneering work, Oger *et al*. (2010) coupled an SPH-based structure solver with a Weakly Compressible version of SPH (WCSPH) for fluid to solve FSI problems including hydroelastic slamming. A challenge in using WCSPH-based fluid modeling in FSI problems corresponds to presence of acoustic perturbations. Recently, Meringolo *et al*. (2017) presented a Wavelet Transform-based filtering technique to accurately filter such acoustic perturbations. In the context of projection-based particle methods, Hwang *et al*. (2014) presented a fully-Lagrangian MPS-based coupled FSI solver and applied it to a number of ocean engineering-related applications including simple hydroelastic slamming and sloshing with elastic baffles (Hwang *et al*. 2015, 2016). The coupling scheme proposed by Hwang *et al*. (2014) was founded on a simple integration of pressure at fluid-structure interface. Hence, the solver could become quite sensitive to even slight fluctuations in pressure field. For this reason, some special treatments, i.e., the so-called grouping scheme, was used in simulations of sloshing with submerged elastic baffle (Hwang *et al*. 2016).

The present study is devoted to development of a reliable, fully-Lagrangian particle-based FSI solver in the framework of MPS method. Our focus is on hydroelastic slamming which is among the important problems encountered in ocean engineering. Accordingly a newly coded MPS-based FSI will be presented in which the fluid model is based on the solution of continuity and Navier-Stokes equations with incorporation of enhanced schemes developed for improvements of stability and accuracy (Gotoh and Khayyer 2016). The projection-based fluid model is carefully coupled with a structure model founded on conservation of linear and angular momenta for an isotropic elastic solid leading to the enhanced KU MPS-MPS FSI (Kyoto University MPS-MPS Fluid Structure

Interaction) method. The fluid-structure coupling is performed in a mathematically-physically consistent manner via utilization of the concept of Helmholtz-Leray decomposition on which the MPS fluid model is founded. The fluid interacting force on structure is modeled directly through a consistent calculation of pressure gradient-related acceleration, instead of applying a simple pressure integration scheme. Performance of the model is verified by a number of benchmark tests including high velocity impact of an elastic aluminum wedge with free surface (Scolan 2004) and hydroelastic slammings of marine panels (Allen *et al*. 2013, Stenius *et al*. 2013). Validations are made both qualitatively and quantitatively in terms of reproduced pressure as well as structure deformation. Several remaining challenges as well as important key issues are highlighted. At last, a recently developed multi-scale MPS method (Tsuruta *et al*. 2016) is incorporated with the developed FSI solver in order to investigate potential adaptivity. The final section of the paper is dedicated to concluding remarks and insights on future research.

2. Numerical method

2.1 Fluid model

The equations of conservation of linear momentum and continuity, as the principle equations for fluid flow modeling are described as follows

$$\left(\frac{D\boldsymbol{u}}{Dt}\right)_F = \frac{1}{\rho_F}\nabla\cdot\boldsymbol{\sigma}_F + \boldsymbol{F}_{S\,to\,F} + \boldsymbol{g} \tag{1}$$

$$\nabla\cdot\boldsymbol{u} = 0 \tag{2}$$

where $\boldsymbol{u}$, ρ_F and t represent velocity vector, density and time for fluid particles (F), respectively, $\boldsymbol{g}$ is the gravitational acceleration and $\boldsymbol{F}_{S\ to\ F}$ corresponds to the interaction force imposed by the neighboring structure particles (S). The stress tensor for a fluid particle, $\boldsymbol{\sigma}_F$, is defined as

$$\boldsymbol{\sigma}_F = -p\boldsymbol{I} + \mu_F\left[\nabla\boldsymbol{u} + (\nabla\boldsymbol{u})^T\right] \tag{3}$$

where p and μ_F stand for pressure and fluid's dynamic viscosity, respectively, and $\boldsymbol{I}$ represents unit tensor.

The continuity is guaranteed with projection of intermediate velocity field into the velocity divergence free condition (Eq. (2)) through solving a Poisson Pressure Equation (Eq. (4)). The MPS-based fluid model benefits from a set of enhanced schemes (Gotoh and Khayyer 2016, Khayyer *et al.* 2017b) developed by authors during the last decade to enhance the stability and accuracy of MPS method. The incorporated enhanced schemes include the so-called HS (Higher-order Source term of PPE; Khayyer and Gotoh 2009), HL (Higher-order Laplacian of PPE; Khayyer and Gotoh 2010), ECS (Error Compensating Source of PPE; Khayyer and Gotoh 2011), GC (Gradient Correction; Khayyer and Gotoh 2011) and DS (Dynamic Stabilization; Tsuruta *et al.* 2013). Following the application of HS (first term on RHS of Eq. (4)) and ECS (second term on RHS of Eq. (4)) schemes, the Poisson Pressure Equation (PPE) is formulated as

$$\left(\frac{\Delta t}{\rho}\nabla^2 p_{k+1}\right)_i = \frac{1}{n_0}\left(\frac{Dn}{Dt}\right)_i^* + \Lambda_{ECS}$$
$$\Lambda_{ECS} = \frac{\alpha}{n_0}\left(\frac{Dn}{Dt}\right)_i^k + \frac{\beta}{\Delta t}\frac{n_i^k - n_0}{n_0} \;;\; \alpha = \left|\frac{n_i^k - n_0}{n_0}\right| \;,\; \beta = \left|\frac{\Delta t}{n_0}\left(\frac{Dn}{Dt}\right)_i^k\right| \tag{4}$$

where n and n_0 denote instantaneous and initial particle number density, respectively, Δt stands for time step size, subscribe i represents target particle and superscripts * and k represent intermediate properties of the fluid and calculation time step number, respectively.

The DS scheme provides minimum required repulsive inter-particle forces to guarantee the stability of the fluid simulation. The DS scheme can be regarded as a particle regularization scheme. A comprehensive discussion is made by Khayyer *et al*. (2017a) on the accuracy and conservation properties of two particle-based regularization schemes, namely, DS and PS (Particle Shifting proposed by Lind *et al*. 2012).

The pressure gradient model is formulated by Eq. (5). Note that this equation incorporates the GC and DS schemes.

$$\left\langle \nabla p \right\rangle_i = \frac{D_s}{n_0}\sum_{j\neq i}\left(p_j - p_i\right)\boldsymbol{C}_i \cdot \boldsymbol{r}_{ij}\frac{w_{ij}}{\left|\boldsymbol{r}_{ij}\right|^2} + \Lambda_{DS} \tag{5}$$

$$\boldsymbol{C}_i = \frac{1}{D_s}\left(\sum_{j\neq i} V_i \frac{\boldsymbol{r}_{ij}\otimes\boldsymbol{r}_{ij}}{\left|\boldsymbol{r}_{ij}\right|^2} w_{ij}\right)^{-1} \;\;;\;\; V_i = \frac{1}{\sum_{j\neq i} w_{ij}} \tag{6}$$

$$\Lambda_{DS} = V_i \sum_{j\neq i} \boldsymbol{F}_{ij}^{DS} w_{ij}$$
$$\begin{cases} \boldsymbol{F}_{ij}^{DS} = 0 & \left|\boldsymbol{r}_{ij}^*\right| \geq d_{ij} \\ \boldsymbol{F}_{ij}^{DS} = -\rho_i \Pi_{ij}\dfrac{\boldsymbol{r}_{ij}}{\left|\boldsymbol{r}_{ij}\right|} & \left|\boldsymbol{r}_{ij}^*\right| < d_{ij} \end{cases} \tag{7}$$
$$\alpha_{dt} = 1.0 - \alpha_{DS} \;;\; d_{ij} = \alpha_{DS}\frac{d_i + d_j}{2}$$
$$\Pi_{ij} = \frac{\rho_j}{(\Delta t)^2\left(\rho_i + \rho_j\right)}\left(\sqrt{d_{ij}^2 - \left|\boldsymbol{r}_{ij\perp}^*\right|^2} - \left|\boldsymbol{r}_{ij\parallel}^*\right|\right)$$

where D_s represents number of space dimensions, $\boldsymbol{C}_i$ denotes Gradient Corrective matrix (Khayyer and Gotoh 2011), $\boldsymbol{r}_{ij} = \boldsymbol{r}_j - \boldsymbol{r}_i$ and $\boldsymbol{r}_i$ is the position vector of target particle i. In Eq. (7), $\boldsymbol{F}_{ij}^{DS}$ is the stabilizing force imposed to target particle i by its neighboring particle j, Π_{ij} is a parameter to adjust the magnitude of $\boldsymbol{F}_{ij}^{DS}$, α_{DS} is a constant for adjusting active range of $\boldsymbol{F}_{ij}^{DS}$, α_{dt} is the ratio of the time step to Courant number used in determination of computational time step (set equal to 0.2 in this study), d_i represents the particle diameter, $\boldsymbol{r}_{ij\parallel}^*$ and $\boldsymbol{r}_{ij\perp}^*$ signify the parallel and normal vectors of $\boldsymbol{r}_{ij}^*$, respectively, i.e., $\boldsymbol{r}_{ij}^* = \boldsymbol{r}_{ij\parallel}^* + \boldsymbol{r}_{ij\perp}^*$.

2.2 Structure model

The structure model is configured according to MPS-based discretization of divergence of stress in Lagrangian form (Eq. (8)). The corresponding constitutive model for the material is considered as Hooke's law with an implicit assumption of linear elasticity (Kondo *et al.* 2007). Accordingly

$$\left(\frac{D\boldsymbol{u}}{Dt}\right)_S = \frac{1}{\rho_S}\nabla\cdot\boldsymbol{\sigma}_S + \boldsymbol{F}_{F\,to\,S} + \boldsymbol{g} \tag{8}$$

$$\boldsymbol{\sigma}_S = \lambda_S tr\left(\boldsymbol{\varepsilon}_S\right)\boldsymbol{I} + 2\mu_S\boldsymbol{\varepsilon}_S \tag{9}$$

where ρ_S stands for density of structure particle, $\boldsymbol{\sigma}_S$ represents the stress tensor of structure particle, $\boldsymbol{\varepsilon}$ is the strain tensor, $\boldsymbol{F}_{F\,to\,S}$ corresponds to the interaction force acting on interface from fluid (F) to structure (S) particles and $\boldsymbol{I}$ symbolizes the unit tensor. Precisely speaking, $\boldsymbol{F}_{F\,to\,S}$ implies the acceleration imposed by fluid particles to structure particles. In Eq. (9), λ_S and μ_S are Lame's constants, i.e., mechanical properties of the material calculated according to Eq. (10) from Young's modulus, E_S, and the Poisson ratio, ν_S (Marsden and Hughes 1983, Slaughter 2002).

$$\lambda_S = \frac{E_S\nu_S}{\left(1+\nu_S\right)\left(1-2\nu_S\right)} \quad ; \quad \mu_S = \frac{E_S}{2\left(1+\nu_S\right)} \tag{10}$$

The conservation of angular momentum is involved into the solution according to Eq. (11) as described by Koshizuka (2005) and Hwang *et al.* (2014).

$$\frac{D}{Dt}I\boldsymbol{\omega} = \frac{D}{Dt}\left(\boldsymbol{r}\times m\boldsymbol{u}\right) \tag{11}$$

where I, $\boldsymbol{\omega}$ and m represent moment of inertia, angular velocity vector and mass of particle, respectively. A 5th order Wendland kernel (Wendland 1995) is applied for weighted-averaging process throughout fluid analysis as well as structure.

2.3 Fluid-structure coupling scheme

In the present study, fluid structure coupling is conducted in a mathematically-physically consistent manner by considering the prediction-correction feature of projection-based particle methods, via extension of the linear momentum equation (Eq. (1)) all over the surrounding particles of the interface either from fluid or structure sub-domains. In other words, structure particles are considered as a moving boundary for the fluid, providing velocity and position boundary conditions in calculation of fluid's pressure field on the basis of momentum and continuity equations. Once the fluid's pressure field is calculated, the acceleration due to hydrodynamic pressure gradient at the fluid-structure interface, namely, $\boldsymbol{F}_{F\,to\,S}$, can be obtained and imposed on the structure. By using this coupling scheme, the interface boundary conditions in between the fluid and structure (Koshizuka, 2005, Antoci *et al.* 2007), i.e.

$$\begin{aligned} \boldsymbol{u}_S &= \boldsymbol{u}_F \\ \boldsymbol{\sigma}_S\,\boldsymbol{n}_S &= -\,\boldsymbol{\sigma}_F\,\boldsymbol{n}_F \end{aligned} \tag{12}$$

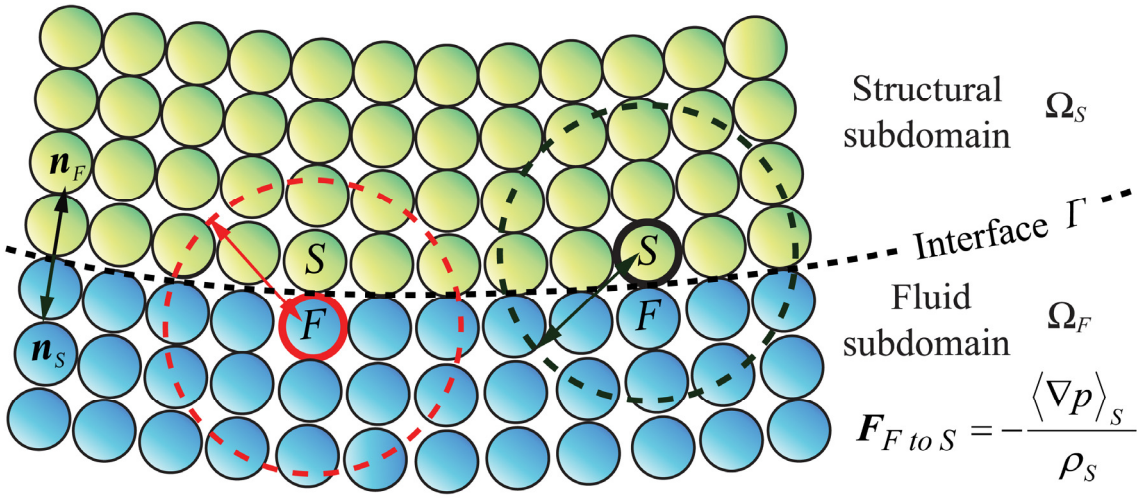

Fig. 1 Schematic sketch of fluid-structure coupling scheme

are satisfied automatically, where, $\boldsymbol{n}_S$ and $\boldsymbol{n}_F$ are normal vectors to structure and fluid interface particles, respectively. Fig. 1 illustrates a schematic sketch of considered FSI coupling scheme.

3. Numerical validations and investigations

In this section, the coupled enhanced MPS-MPS FSI solver is applied to simulations of a set of benchmark tests, namely, high velocity impact of an elastic aluminum wedge (Oger *et al*. 2010, Scolan 2004) and hydroelastic slammings of marine panels (Allen 2013, Stenius *et al*. 2013) to investigate its performance and reliability.

3.1 High velocity impact of an elastic aluminum wedge

The proposed FSI solver is verified in simulation of the impact of an elastic wedge on free surface as illustrated in Fig. 2 corresponding to the study by Scolan (2004). Scolan (2004) investigated the hydroelastic effects by coupling a hydrodynamic Wagner model to a linear model of elasticity for thin shells. The deformable beam wedge with the length of L = 0.6 m and thickness of δ = 0.04 m, directs downward and finally hits the free surface with a dead-rise angle of β = 10° and a constant velocity of u = 30 m/s (u is in vertical direction). According to the theory, all the degrees of freedom are restrained at the center of the wedge as well as the extremities. The Young's modulus and Poisson ratio of aluminum beam wedge are set as E = 67.5 GPa and v = 0.34, respectively.

This slamming benchmark test is reproduced by considering a set of particle diameters, namely, δ/d_0 = 3, 4 and 5 (with δ being the panel thickness and d_0 being the particle size). Figs. 3(a)-3(d) illustrates the snapshots of particles together with pressure and stress fields for the case of δ/d_0 = 5. As it can be seen from the presented figure, the developed MPS-based FSI solver has produced smooth and qualitatively acceptable pressure and stress fields in fluid and structure partitions, respectively. Another important feature that can be realized from the presented set of snapshots

corresponds to geometrical continuity of fluid and structure particles (and absence of an unphysical gap in between fluid and structure particles often seen in FSI simulations). This is an important issue in FSI simulations and is achieved thanks to an integrated fully-Lagrangian modeling as well as implementation of a consistent coupling scheme in the framework of MPS method.

Fig. 4 portrays the convergence properties of developed FSI solver. From this figure, refinement of spatial resolution has resulted in better agreements in between simulation results and the experiment in terms of deflection, d, of the wedge at point C. For the case of particle diameter corresponding to $\delta/d_0 = 5$, the calculated time history of deflection agrees well with the semi-analytical solution by Scolan (2004).

Fig. 5 presents time histories of calculated pressure at measuring points A-D along with their corresponding semi-analytical solutions (Scolan 2004) for the case of $\delta/d_0 = 5$. Despite presence of some small-scale levels of pressure oscillations, the agreement in between obtained numerical results and semi-analytical pressures is acceptable. In particular, the developed FSI solver has provided quite accurate estimations of the instants of peak pressures despite presence of slight level of discrepancies in calculated pressure magnitudes. By further refinements of differential operator models incorporated in fluid and structure models such small-scale pressure oscillations are expected to be minimized and the accuracy of the MPS-based FSI solver should be further enhanced.

In addition to incompleteness/imprecision of differential operator models, other sources of discrepancies in between numerical and semi-analytical results (observed in Fig. 5), can be attributed to possible incidences of so-called zero-energy modes (Randles and Libersky 2000, Rabczuk *et al.* 2004) as well as incorporation of a simple explicit time integration scheme for structure model. As for occurrence of zero-energy modes, this is the case for collocation-based structure models where physical properties and their derivatives are being calculated at the same computational points. Stress-point integration scheme (Randles and Libersky 2000) can be considered to resolve the issue related to zero-energy modes. As for time integration, higher order implicit schemes can be adopted (e.g., Bathe and Irfan Baig 2005).

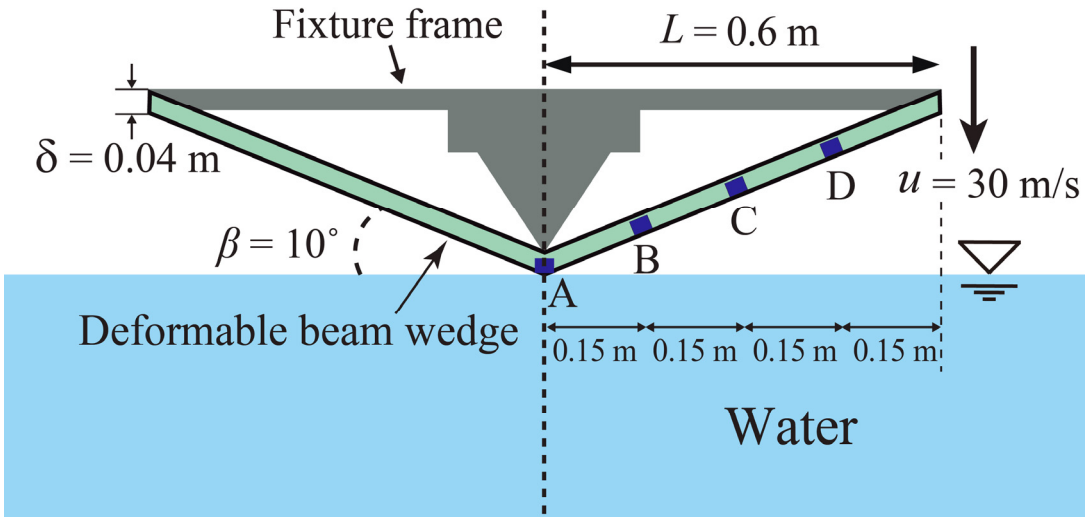

Fig. 2 Schematic illustration of the initial set up of the benchmark test of high velocity impact of an elastic aluminum wedge (Scolan 2004, Oger *et al.* 2010)

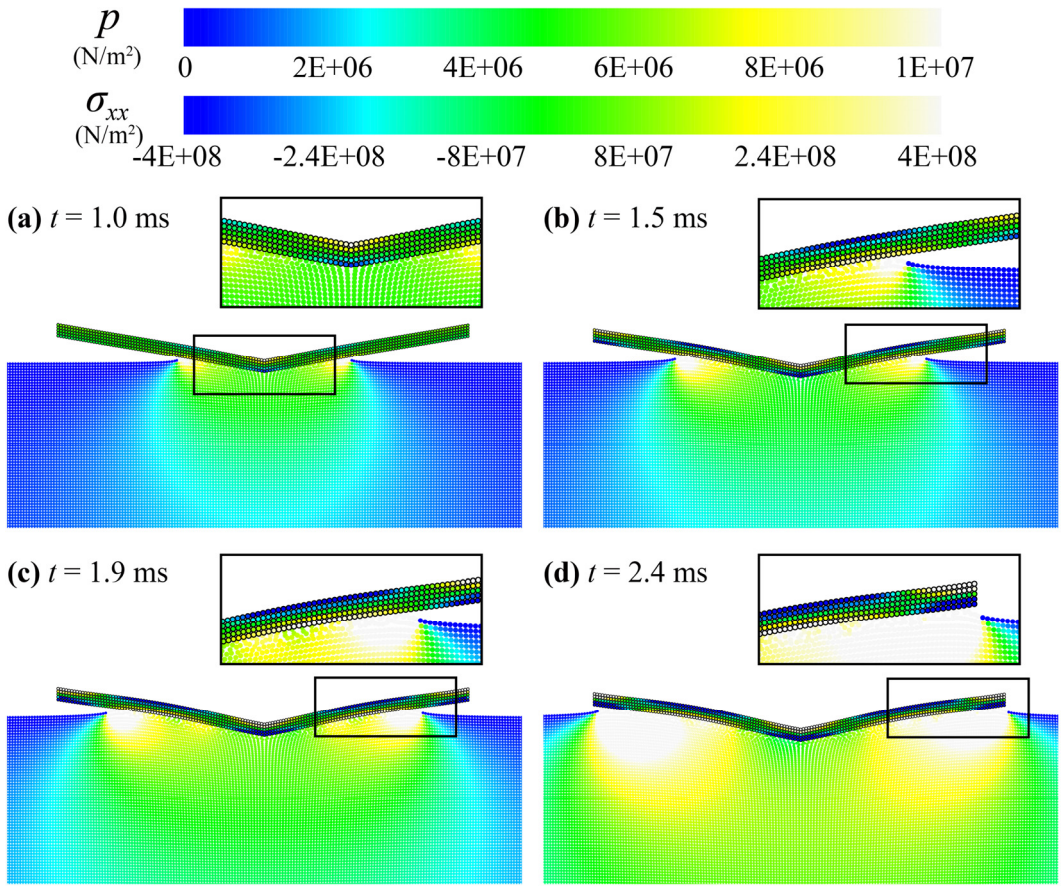

Fig. 3 Snapshots of stress (σ_{xx}) / pressure (p) fields reproduced by enhanced KU MPS-MPS method in high velocity impact of an elastic aluminum wedge (Scolan 2004) in case of u = 30 m/s, (a) t = 1.0 ms, (b) t = 1.5 ms, (c) t = 1.9 ms and (d) t = 2.4 ms, respectively

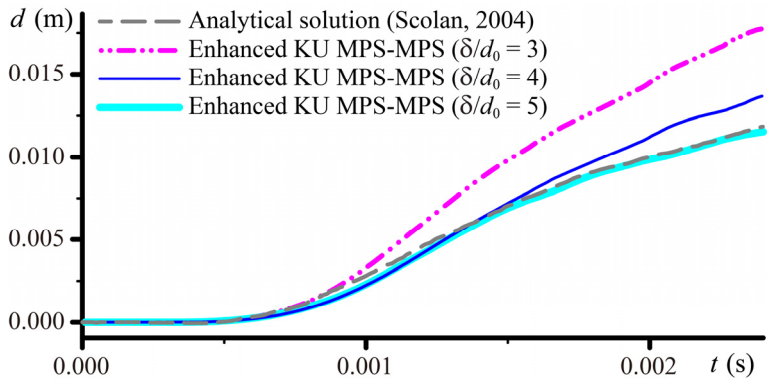

Fig. 4 Convergence study on the time history of deflection (d) of deformable wedge at measuring point C; results by enhanced KU MPS-MPS method using particle diameters corresponding to δ/d_0 = 3, 4 and 5 together with semi-analytical solution by Scolan (2004) – impact of an elastic aluminum wedge

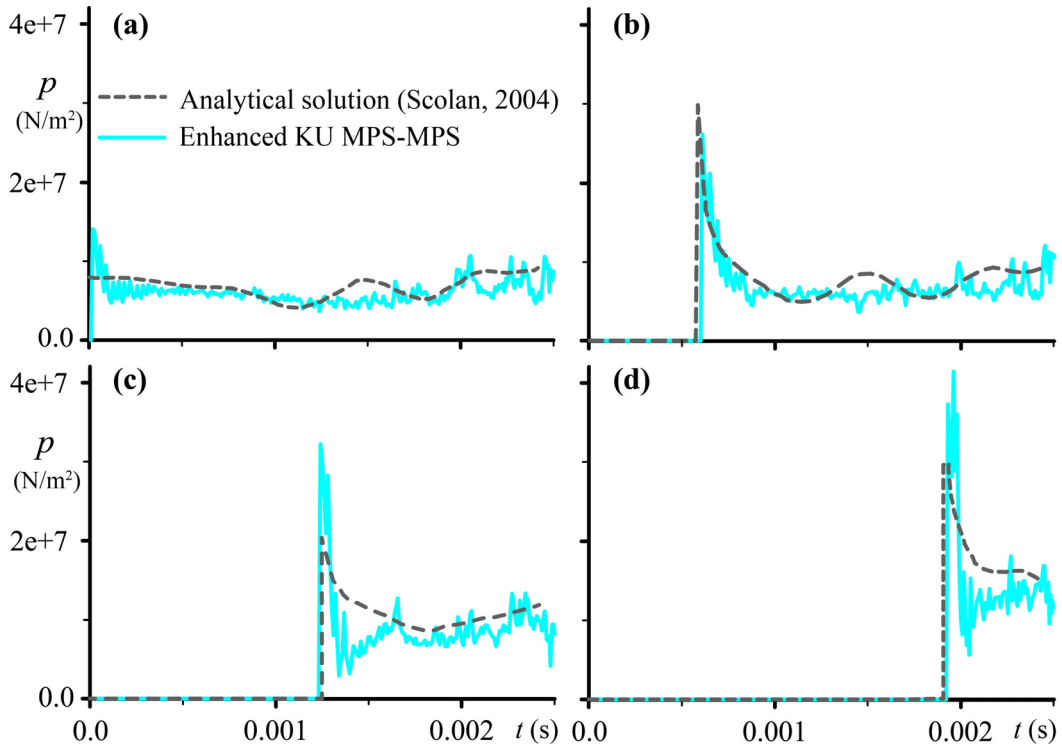

Fig. 5 Pressure at measuring points (a) A, (b) B, (c) C and (d) D, results by enhanced KU MPS-MPS method for $\delta/d_0 = 5$ – impact of an elastic aluminum wedge (Scolan 2004)

3.2 Hydroelastic slammings of marine panels

In this section, the developed fully-Lagrangian MPS-based FSI solver is applied for simulation of hydrodynamic slamming tests of marine panels corresponding to experiments by Allen (2013). Fig. 6(a) illustrates a schematic sketch of the experimental set up. The experiments were conducted using a Servo-hydraulic Slam Testing System (SSTS) in a water tank of 3.5 m diameter and 1.4 m depth. Present numerical study targets two test cases of interest i.e., Solid Glass fiber single skin panel (SG panel) (Allen 2013, Stenius *et al.* 2013) and deformable foam-cored sandwich panel (Gurit® M100) with skins of GPR (GM100 panel) (Allen 2013, Camilleri *et al.* 2015). Detailed material data and configuration of each panel are described in Table 1 and Figs. 6(b) and 6(c), respectively. The panels were being carried on a rig capable of driving either with constant or variable velocities in the range of dead-rise angles from 0° up to 40°. The extremities of the panels were simply supported by a fixture frame, setting an unsupported area of 0.99 m by 0.485 m (GM100 panel) or 0.495 m (SG panel) between the simply supported edges of the test fixture. The lower supported edge was representative of keel while the upper as chine. The instrumentation was capable of measuring dynamic pressure as well as displacement through a set of transducers. Note that GM100 panel is composed of one thick medium and two thin stiffer skin, resulting in a challenge

for numerical simulation especially in the context of particle methods. Therefore, a simplification is tested here for simulation of a composite GM100 panel, that approximates a sandwich panel with a mechanically equivalent homogeneous one. The conceptual scheme is portrayed in Fig. 6(d). Based on the aforementioned simplification, the equivalent homogeneous panel is assumed to possess Young's modulus and Poisson's ratio as E = 11.29E+09 N/m^2 and υ = 0.3, respectively, that exactly correspond to the skins of the composite GM100 panel. Accordingly and in order to attain an equivalent bending stiffness with respect to that of the composite GM100 panel (i.e., 2.54 kNm, Table 1), the thickness of equivalent homogeneous panel is set as 14 mm. Also, the density of equivalent panel is set as 520.11 kg/m^3, resulting in the same total weight as that of composite GM100 panel (i.e., 4.5 kg). Hence, the homogeneous panel would have the same bending stiffness and total weight as those of the composite GM100 panel.

In regards to the experimental constraint conditions, the panel is fixed against the test frame using fabric straps and steel fittings preventing in-plane strain (Stenius *et al*. 2013). In case of 3D simulations, in order to achieve the consistency with the constraint conditions of the experiment, the panel should be fixed in terms of all degrees of freedom at four points while constrained in four marginal lines excluding the in-plane strains (Stenius *et al*. 2013). For 2D simulations, which is the case for the present study, the panel is restrained at two points leading to a free span representing the inner edges of the fixture frame. The edges of the panel are restrained in vertical direction while the in-plane strain is restrained at chine edge (Camilleri *et al.* 2015). In order to achieve consistency with experimental conditions, the restraining particles are set outside of the panel as shown in Fig. 7, representing a realistic physical condition of fixture frame. It must be highlighted here that proper consideration and implementation of boundary conditions play a crucial role to achieve a reliable simulation with consistent deflection and pressure time histories.

Figs. 8(a)-8(d) portrays a set of representative snapshots corresponding to the test case of SG panel slamming the water surface with a downward vertical velocity of 4 m/s. As it can be seen in this figure, the developed particle-based FSI solver has performed well in reproducing smooth pressure field in fluid as well as stress field in the structure. The achieved results are qualitatively acceptable, meanwhile, the reliability of developed FSI solver must be investigated quantitatively and preferably in terms of reproduced pressure, deflection and stress.

Figs. 9(a) and 9(b) depict a quantitative comparison of time histories of deflection at transducer D3 for the case of u = 4 m/s and pressure at transducer P3 for the case of u = 3 m/s with experimental results by Allen (2013) and semi-empiric model of Stenius *et al*. (2013). Fig. 9(a) shows that reproduced deflection by the enhanced KU MPS-MPS at D3 is in good agreement with that in the experiment. In addition, the deflection time history by the developed solver is in a clear closer agreement with the experiment in comparison to the semi-empiric model of Stenius *et al.* (2013).

Table 1 Hydroelastic slamming test conditions for SG and GM100 marine panels

	Thickness (mm)	Bending stiffness (kNm)	Shear stiffness (kN/m)	Tested velocities (m/s)
GM100	t_s* = 1.63 t_c ** = 14.0	2.54	722	1.0
SG	9.5	1.52	44.0E+03	3.0 and 4.0

* thickness of the skins of sandwich panel
** thickness of the core of sandwich panel

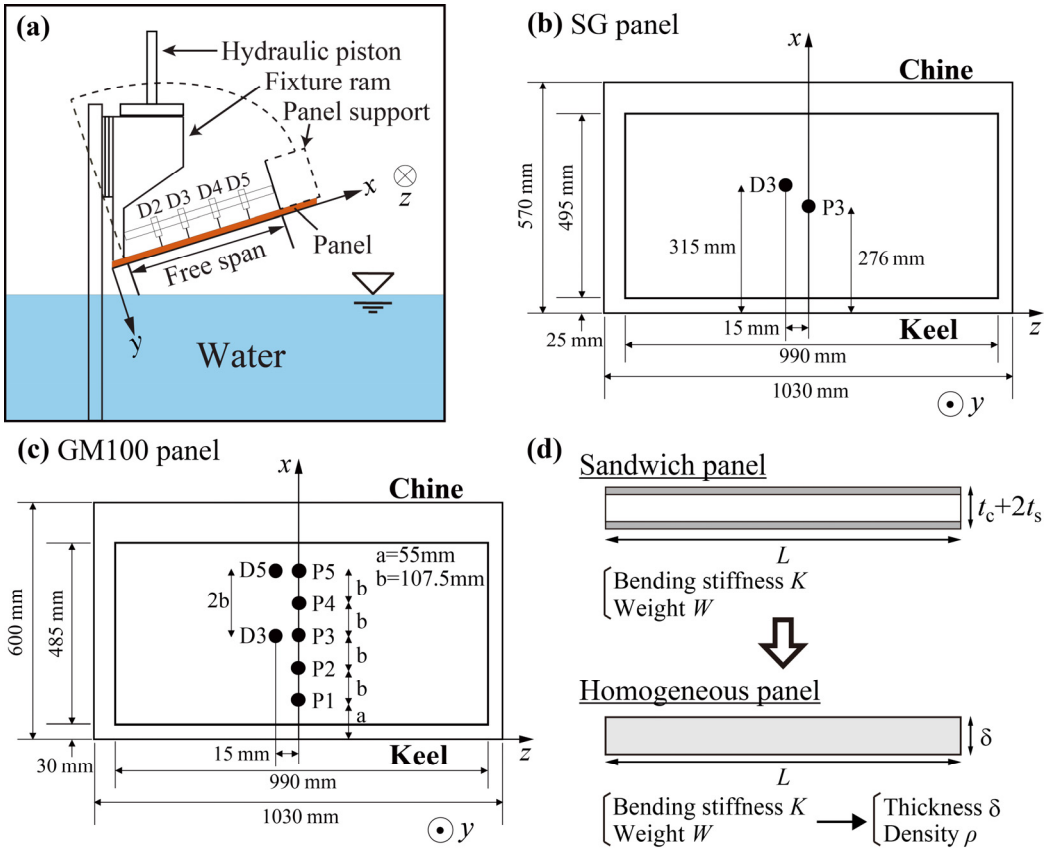

Fig. 6 Set up of the benchmark test of hydroelastic slammings of marine panels (Allen 2013, Stenius *et al.* 2013); (a) schematic sketch of Servo-hydraulic Slam Testing System (SSTS), (b,c) configuration of SG panel and GM100 panel with pressure transducers (P1-P5) and deflection transducers (D3, D5), (d) schematic sketch of sandwich panel (GM100) simplification

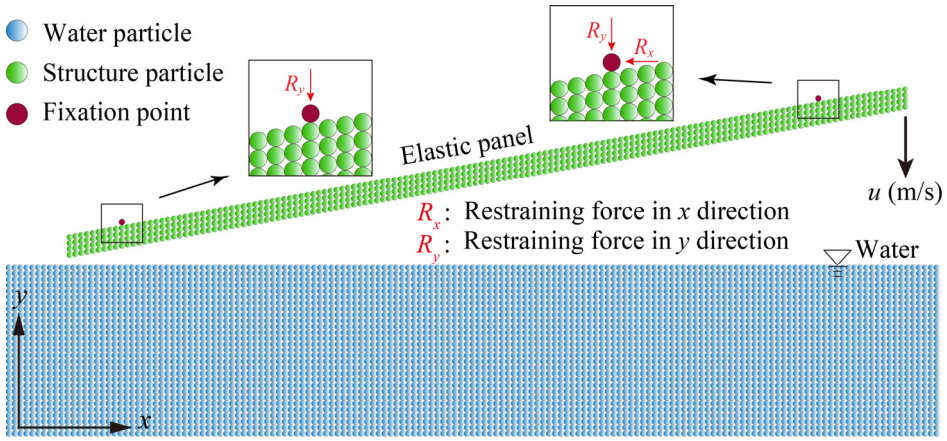

Fig. 7 Schematic sketch of the fixation particles and restraining conditions (Allen 2013, Camilleri *et al.* 2015)

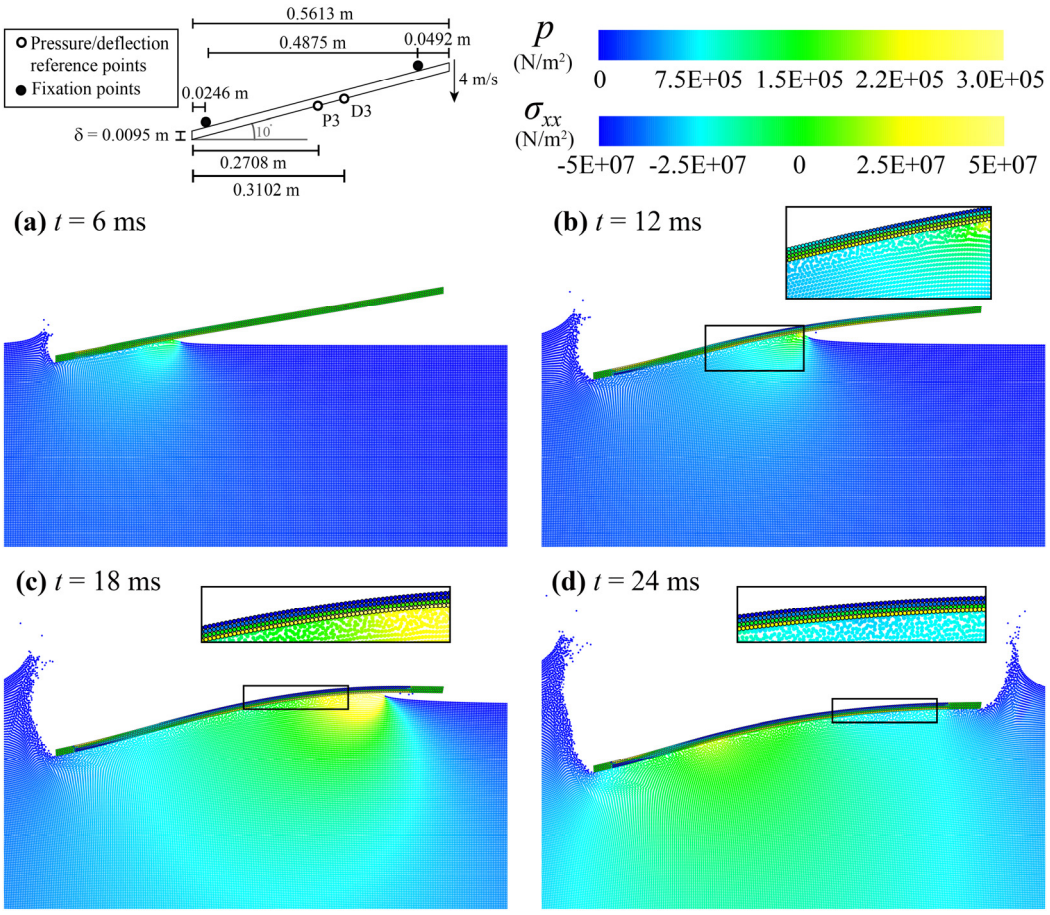

Fig. 8 Snapshots of the stress (σ_{xx}) / pressure (p) fields reproduced by the enhanced KU MPS-MPS method in hydroelastic slamming test of SG panel in case of u = 4 m/s; (a) t = 6 ms, (b) t = 12 ms, (c) t = 18 ms and (d) t = 24 ms – hydroelastic slammings of marine panels (Allen 2013)

From Fig. 9(b) the reproduced pressure time history at P3 is found to be in a moderately acceptable agreement with the experiment, especially with respect to the instant of peak pressure. It must be noted that there are also certain sources of uncertainties in the experiments considering the complicated nature of the targeted problem. Meanwhile, continuous efforts must be made to further enhance the accuracy of the developed FSI solver and further validations and numerical investigations must be conducted by considering other available experiments related to hydroelastic slamming.

Figs. 10(a) and 10(b) present a set of snapshots corresponding to the test case of GM100 panel that slams the water surface with a velocity of 1 m/s. From the presented figure, the developed FSI solver has provided qualitatively accurate results similar to previous performed simulations.

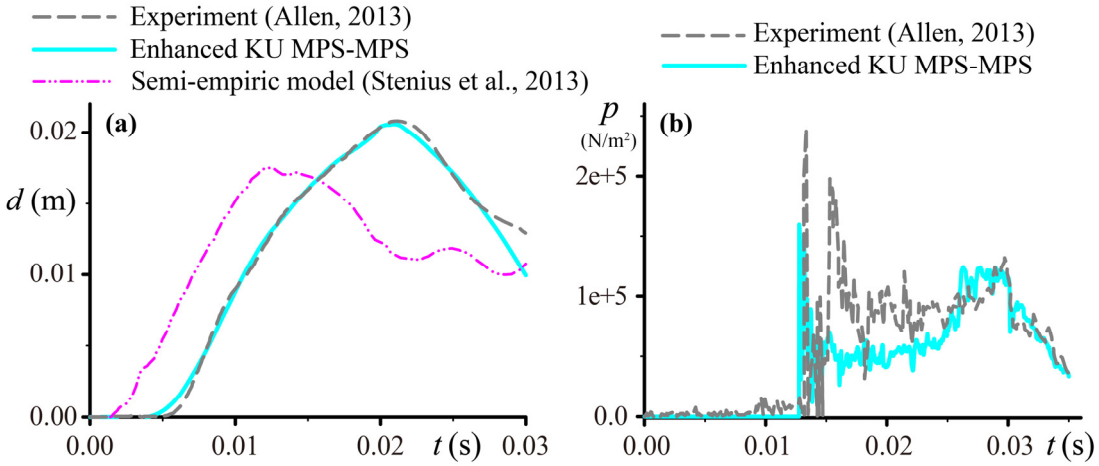

Fig. 9 Quantitative analysis of hydroelastic slamming of SG panel; results by enhanced KU MPS-MPS method, semi-empiric rigid quasi-static model of Stenius *et al.* (2013) and experiment (Allen 2013); (a) Deflection (d) at D3 in case of $u = 4$ m/s, (b) pressure at P3 in case of $u = 3$ m/s – hydroelastic slammings of marine panels (Allen 2013)

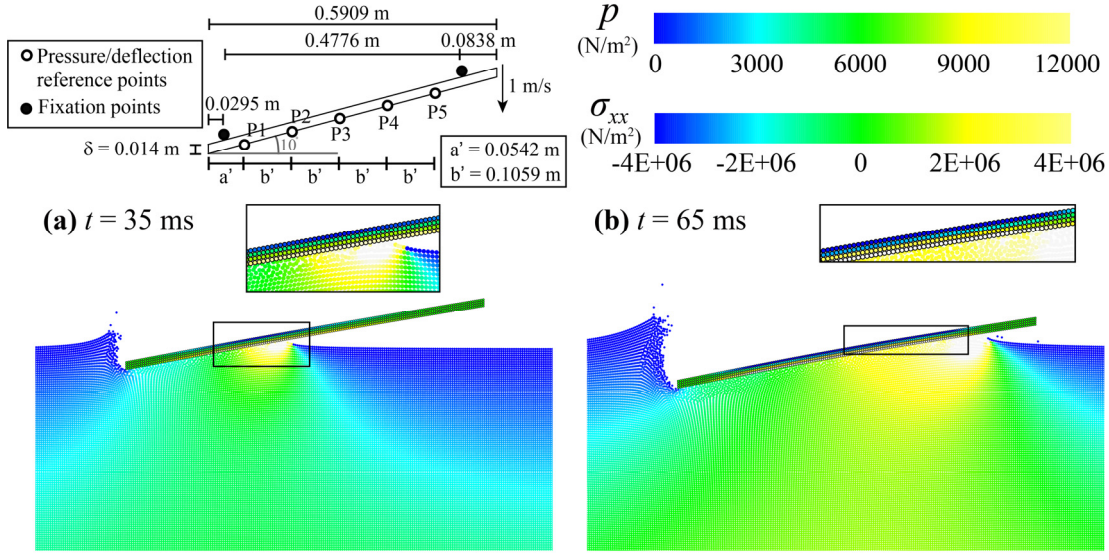

Fig. 10 Snapshots of the stress (σ_{xx}) / pressure (p) fields reproduced by enhanced KU MPS-MPS method in hydrodynamic slamming test of GM100 panel in case of $u = 1$ m/s; (a) $t = 35$ ms and (b) $t = 65$ ms – hydroelastic slammings of marine panels (Allen 2013)

Figs. 11(a) and 11(b) illustrate the deflections at transducers D3 and D5, obtained from present MPS-based FSI solver in comparison with those obtained from the experiment (Allen 2013) as well as the coupled FVM-FEM solver of Camilleri *et al.* (2015). From the presented figures, the MPS-based FSI solver is found to have acceptable convergence property and to perform relatively well in reproduction of the hydroelasticity effects in slamming loaded GM100 panel. The observed discrepancies, in particular those corresponding to pressure time histories, are expected to be minimized through a more realistic modeling of GM100 panel as well as incorporation of further refined differential operator models for the MPS-based FSI solver.

Fig. 11(c) presents a comparison in terms of the time histories of pressure at transducers P1 to P5 reproduced by developed FSI solver against those obtained from the experiment. From this figure, the instants of peak pressures are overestimated and their magnitudes are mainly underestimated.

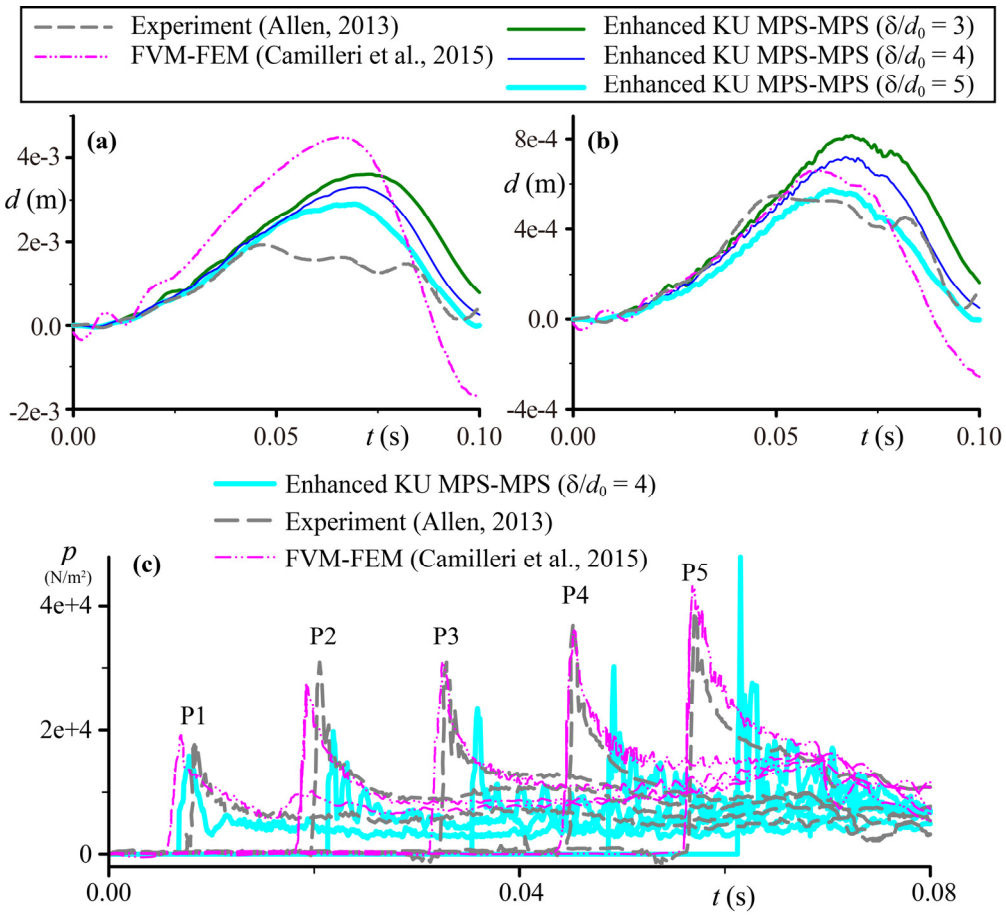

Fig. 11 Quantitative analysis of hydroelastic slamming of GM100 panel in case of u = 1 m/s; results by enhanced KU MPS-MPS method, FVM-FEM method of Camilleri *et al.* (2015) and experiment (Allen 2013); (a) Deflection (d) time history at D3, (b) Deflection (d) time history at D5 and (c) pressure time history at P1-P5 for the simulation case of δ (panel thickness)/d_0 (particle diameter) = 4 – hydroelastic slammings of marine panels (Allen 2013)

This is likely due to the simplification of the sandwich panel by a homogeneous one. The density of the homogeneous panel is set smaller than that of original skin to keep the overall weight the same, leading to smaller source term in PPE and thus, smaller pressures.

The smaller density of panel considered in the simulation is likely one of the main causes for larger deformations obtained even with smaller pressures. Indeed, a more consistent modeling of the composite sandwich panels should be conducted to minimize the existing discrepancies. In this regard, proper treatment of the material interface discontinuity is a key issue.

4. Towards development of a multi-resolution FSI solver

A challenge in simulation of practical FSI problems, including those related to hydroelastic slamming, corresponds to requirements on computational cost as well as Random Access Memory, RAM.

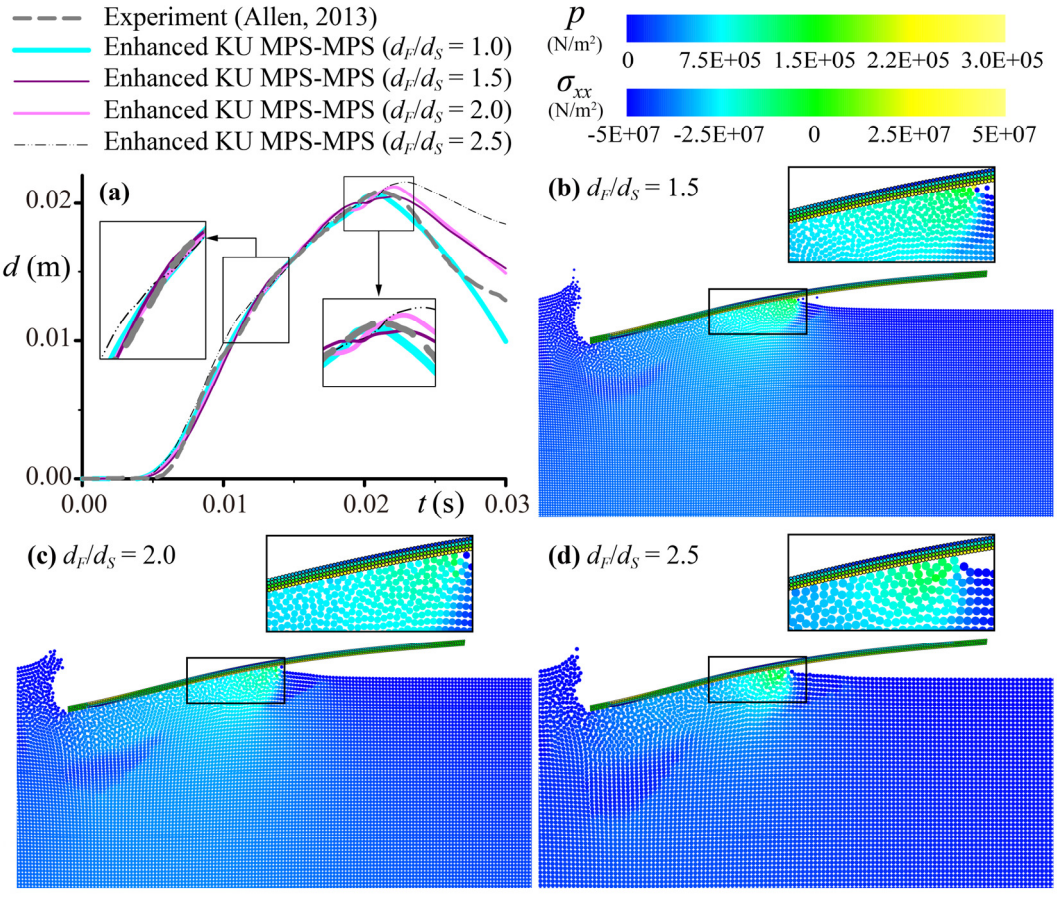

Fig. 12 Time history of deflection (d) at D3 (a), and snapshots of the stress (σ_{xx}) / pressure (p) fields at t = 12.0 ms with different diameter ratios (b)-(d) reproduced by the enhanced KU MPS-MPS method in hydrodynamic slamming test on SG panel in case of u = 4 m/s – hydroelastic slammings of marine panels (Allen 2013)

This challenge becomes more pronounced in 3D simulations as well as cases where very fine structural elements are supposed to be modeled. In most cases, fine spatial resolutions are required at and in the vicinity of fluid-structure interface. Moreover, with respect to the substantial differences in between fluid and structural dynamics as well as the computational solution procedure (semi-implicit for fluid vs. explicit for structure), the scale of refinement in fluid analysis should differ from that of structure. Hence, the so-called adaptivity of the proposed FSI solver would attain a great importance such that variable resolutions can be considered for the fluid and structure. It must be noted here that adaptivity is regarded as one of the grand challenges of particle methods by the SPHERIC (SPH European Research Interest Community).

Here a preliminary extension of the proposed FSI solver into an adaptive multi-resolution one is investigated. The considered multi-resolution scheme corresponds to that proposed by Tsuruta et al. (2016) for MPS-based simulations of fluid flows. In this multi-resolution (or multi-scale) MPS method, a common domain of influence is employed for all the scales of particle refinement in order to guarantee the momentum conservation. Accordingly, a modified kernel function and particle number density are presented in this multi-resolution framework.

In this section, adaptivity of the multi-resolution enhanced KU MPS-MPS method is investigated through simulations of the hydroelastic slamming test related to the SG panel. Three additional sets of resolutions with diameter ratios of d_F/d_S = 1.5, 2.0 and 2.5 are considered (d_F and d_S represent the diameter of fluid particle and diameter of structure particle, respectively).

Fig. 12(a) presents the time history of deflection (d) at D3. From this figure, for all diameter ratios almost acceptable agreements are achieved and results gradually approach the experiment as d_F/d_S is decreased. Indeed, the best agreement corresponds to d_F/d_S = 1.0 where same resolutions are considered for fluid and structure. However, even for the case of d_F/d_S = 2.5 which requires a considerably smaller computational time, an almost acceptable deflection time history is obtained.

Figs. 12(b)-12(d) present a set of snapshots illustrating the stress (σ_{xx}) / pressure (p) fields at t = 12.0 ms by the multi-resolution FSI solver. The snapshots portray a qualitatively acceptable performance of the multi-resolution KU MPS-MPS solver. In particular, stable and smooth pressure/stress fields are achieved and as seen in Fig. 12(a) the results seem to be quantitatively verified as well. Hence, after conducting a set of more careful investigations and validations, the proposed solver which is currently being developed can be comprehensively presented and can be then applied for practical hydroelastic slamming simulations.

5. Conclusions

The paper presents the ongoing efforts towards development of a reliable multi-resolution fully-Lagrangian solver for simulation of hydroelastic slamming. The solver is developed within the framework of Moving Particle Semi-implicit (MPS) method which is a well-known projection-based particle method. The fluid model is founded on the solution of continuity and Navier-Stokes equations. A set of refined schemes are incorporated to enhance the stability and accuracy of the fluid model. The structure model is based on conservations of linear and angular momenta for an isotropic elastic solid. The fluid and structure coupling scheme is consistently performed thanks to the semi-implicit projection-based feature of MPS. The developed Fluid-Structure Interaction (FSI) solver is referred to as enhanced KU (Kyoto University) MPS-MPS method.

The developed solver is first validated through the simulation of a high velocity impact of an aluminum wedge for which semi-analytical solutions exist (Scolan 2004). Then, several sets of

hydroelastic slamming simulations corresponding to the marine panel slamming experiments by Allen (2013) are performed. The performance of the developed FSI solver is found to be almost acceptable for the case of a homogenous SG (Stained-Glass) panel where acceptable deflection and pressure time histories are obtained. An existing challenge corresponds to simulation of composite sandwich panels (GM100) due to presence of material discontinuities that require special treatments, especially in the context of particle methods. In this paper, an investigation is made by simply modeling the sandwich panel by a mechanically equivalent homogeneous one that has the same overall weight and bending stiffness. The obtained results are found to be of moderate agreements with the experiment despite existence of discrepancies. In this regard, further developments and enhancements are required.

The overall performance of the developed MPS-based FSI solver is found to be acceptable in terms of stability and accuracy. In particular, the achieved results are characterized by smooth pressure/stress fields, continuity of fluid-structure particle distributions as well as almost accurate pressure/deflection time histories. It must be noted here that the proposed solver does not take in any artificial numerical stabilizers, and stability is guaranteed through development and incorporation of mathematically-physically consistent schemes. The simulation-experiment agreement is also found to outperform those corresponding to semi-empirical or other numerical models.

As a preliminary investigation on adaptivity of the KU MPS-MPS FSI solver, a recently developed multi-resolution MPS scheme (Tsuruta *et al.* 2016) is considered, resulting in an ongoing development of a multi-resolution FSI solver for hydroelastic slamming simulations. The preliminary results are found to be quite promising although more careful and rigorous investigations/developments must be made. Hence, followed by a set of more detailed investigations and rigorous validations, the proposed FSI solver which is currently being developed can be comprehensively presented and can then be applied for practical hydroelastic slamming simulations.

Other ongoing and future works correspond to extension of the solver to three dimensions, development of multi-phase air-water-structure model and incorporation of SPS (Sub-Particle-Scale; Gotoh *et al.* 2001) turbulence modeling. As for modeling of air phase, an existing challenge corresponds to presence of air-water (or air-structure) large density ratio (Khayyer and Gotoh 2013) as well as proper modeling of air compressibility (Khayyer and Gotoh 2016). We expect that our ongoing efforts would lead to a reliable, accurate and consistent multi-scale, multi-physics computational method for practical simulations of FSI problems, especially those encountered in coastal and ocean engineering.

References

Allen, T. (2013), "Mechanics of flexible composite hull panels subjected to water impacts", Ph.D. Dissertation, University of Auckland, New Zealand.

Aly, A.M., Asai, M., and Sonoda, Y. (2011), "Simulation of free falling rigid body into water by a stabilized incompressible SPH method", *Ocean Syst. Eng.*, **1**(3), 207-222.

Antoci, C., Gallati, M. and Sibilla, S. (2007), "Numerical simulation of fluid–structure interaction by SPH", *Comput. Struct.*, **85**, 879-890.

Aquelet, N. and Souli, M. (2003), "Damping effect in fluid–structure interaction: application to slamming problem", *Proceedings of the ASME Pressure Vessel and Piping Conference*, Cleveland, OH, USA.

Bathe, K.J. and Irfan Baig, M.M. (2005), "On a composite implicit time integration procedure for nonlinear dynamics", *Comput. Struct.*, **83**, 2513-2524.

Camilleri, J., Temarel, P. and Taunton, D. (2015), "Two-dimensional numerical modelling of slamming impact loads on high-speed craft", *Proceedings of the 7th International Conference on Hydroelasticity in Marine Technology Split*, Croatia.

Campbell, J.C., Vignjevic, R. and Patel, M. (2010), "Modelling fluid–structure impact with the coupled FE-SPH approach", *Proceedings of the William Froude Conference on Advances in Theoretical and Applied Hydrodynamic*, Portsmouth, UK.

Das, K. and Batra, R. (2011), "Local water slamming impact on sandwich composite hulls", *J. Fluid. Struct.*, **27**, 523-551.

De Backer, G., Vantorre, M., Beels, C., De Pré, J., Victor, S., De Rouck, J., Blommaert, C. and Van Paepegem, W. (2009), "Experimental investigation of water impact on axisymmetric bodies", *Appl. Ocean Res.*, **31**, 143-156

Faltinsen, O.M. (1999), "Water entry of a wedge by hydroelastic orthotropic plate theory", *J. Ship Res.*, **43**, 180-193.

Faltinsen, O.M. (2002), "Water entry of a wedge with finite deadrise angle", *J. Ship Res.*, **46**, 39-51.

Fourey, G., Oger, G., Le Touzé, D. and Alessandrini, B. (2010), "Violent Fluid-Structure Interaction simulations using a coupled SPH/FEM method", *IOP Conf. Series: Materials Science and Engineering*, **10**, 012041.

Gingold, R.A. and Monaghan, J.J. (1977). "Smoothed particle hydrodynamics – theory and application to non-spherical stars", *Mon. Not. R. Astron. Soc*., **181**, 375-389.

Gotoh, H. and Khayyer, A. (2016), "Current achievements and future perspectives for projection-based particle methods with applications in ocean engineering", *J. Ocean Eng. Mar. Energy*, **2**, 251-278.

Gotoh, H., Shibahara, T. and Sakai, T. (2001) "Sub-particle-scale turbulence model for the MPS method-Lagrangian flow model for hydraulic engineering", *Comput. Fluid Dyn.*, **9**(4), 339-347.

Hwang, S.C., Khayyer, A., Gotoh, H. and Park, J.C. (2014), "Development of a fully Lagrangian MPS-based coupled method for simulation of fluid-structure interaction problems", *J. Fluid. Struct.*, **50**, 497-511.

Hwang, S.C., Khayyer, A., Gotoh, H. and Park, J.C. (2015), "Simulations of incompressible fluid flow-elastic structure interactions by a coupled fully Lagrangian solver", *Proceedings of the 25th International Ocean and Polar Engineering Conference Kona*, Big Island, Hawaii, USA.

Hwang, S.C., Park, J.C., Gotoh, H., Khayyer, A. and Kang, K.J. (2016), "Numerical simulations of sloshing flows with elastic baffles by using a particle-based fluid–structure interaction analysis method", *Ocean Eng.*, **118**, 227-241.

Khayyer, A. and Gotoh, H. (2009), "Modified moving particle semi-implicit methods for the prediction of 2D wave impact pressure", *Coast. Eng*., **56**, 419-440.

Khayyer, A. and Gotoh, H. (2010), "A higher order Laplacian model for enhancement and stabilization of pressure calculation by the MPS method", *Appl. Ocean Res.*, **32**, 124-131.

Khayyer, A. and Gotoh, H. (2011), "Enhancement of stability and accuracy of the moving particle semi-implicit method", *J. Comput. Phys.*, **230**, 3093-3118.

Khayyer, A. and Gotoh, H. (2013), "Enhancement of performance and stability of MPS meshfree particle method for multiphase flows characterized by high density ratios", *J. Comput. Phys.*, **242**, 211-233.

Khayyer, A. and Gotoh, H. (2016), "A multiphase compressible-incompressible particle method for water slamming", *Int. J. Offshore Polar.*, **26**(1), 20-25.

Khayyer, A., Gotoh, H. and Shimizu, Y. (2017a), "Comparative study on accuracy and conservation properties of two particle regularization schemes and proposal of an optimized particle shifting scheme in ISPH context", *J. Comput. Phys.*, **332**, 236-256.

Khayyer, A., Gotoh, H., Shimizu, Y. and Gotoh, K. (2017b), "On enhancement of energy conservation properties of projection-based particle methods", *Eur. J. Mech. B/Fluids*, **66**, 20-37.

Kondo, M., Tanaka, M., Harada, T. and Koshizuka, S. (2007), "Elastic objects for computer graphic field using MPS method", *ACM SIGGRAPH 2007 poster (p. 53). ACM.*, San Diego, USA.

Koshizuka, S. (2005), *Ryushiho (Particle Method)*, Maruzen, Japan (in Japanese).

Koshizuka, S. and Oka, Y. (1996), "Moving particle semi-implicit method for fragmentation of incompressible fluid", *Nuclear. Sci. Eng.*, **123**, 421-434.

Lind S.J., Xu R., Stansby P.K. and Rogers B.D. (2012), "Incompressible smoothed particle hydrodynamics for free-surface flows: a generalised diffusion-based algorithm for stability and validations for impulsive flows and propagating waves", *J. Comput. Phys.*, **231**(4), 1499-1523.

Lind, S.J., Stansby, P.K., Rogers, B.D. and Lloyd, P.M. (2015), "Numerical predictions of water–air wave slam using incompressible–compressible smoothed particle hydrodynamics", *Appl. Ocean Res.*, **49**, 57-71.

Liu, W., Wu, W. and Suzuki, K. (2015), "Dynamic strength of a ship based on 2D hydroelasto-plasticity and FEM in extreme waves", *Proceedings of the 25th International Ocean and Polar Engineering Conference Kona*, Big Island, Hawaii, USA.

Lucy, L.B. (1977), "A numerical approach to the testing of fission hypothesis", *Astronom. J.*, **82**, 1013-1024.

Marsden, J.E. and Hughes, T.J.R. (1983), "Mathematical Foundations of Elasticity", Prentice Hall: Englewood Cliffs, NJ, ISBN 0-486-67865-2, 556.

Meringolo, D.D., Colagrossi, A., Marrone, S. and Aristodemo, F. (2017), "On the filtering of acoustic components in weakly-compressible SPH simulations", *J. Fluid. Struct.*, **70**, 1-23.

Oger, G., Guilcher, P.M., Jacquin, E., Brosset, L., Deuff, J.B. and Le Touzé, D. (2010), "Simulations of hydro-elastic impacts using a parallel SPH model", *Int. J. Offshore Polar.*, **20**(3), 181-189.

Panciroli, R., Abrate, S., Minak, G. and Zucchelli, A. (2012), "Hydroelasticity in water-entry problems: comparison between experimental and sph results", *Compos. Struct.*, **94**, 532-539.

Peseux, B., Gornet, L. and Donguy, B. (2005), "Hydrodynamic impact: numerical and experimental investigations", *J. Fluid. Struct.*, **21**, 277-303.

Rabczuk, T., Belytschko, T. and Xiao, S.P. (2004), "Stable particle methods based on Lagrangian kernels", *Comput. Method. Appl. Mech.*, **193**, 1035-1063.

Randles, P.W. and Libersky, L.D. (2000), "Normalized SPH with stress points", *Int. J. Numer. Meth. Eng.*, **48**, 1445-1462.

Scolan, Y.M. (2004), "Hydro-elastic behavior of a conical shell impacting on a quiescent-free surface of an incompressible liquid", *J. Sound Vib.*, **277**, 163-203.

Slaughter, W.S. (2002), "The linearized theory of elasticity", Springer Science + Business Media, LLC, New York, ISBN 978-1-4612-6608-2, 543.

Stenius, I., Rosén, A., Battley, M. and Allen, T. (2013), "Experimental hydroelastic characterization of slamming loaded marine panels", *Ocean Eng.*, **74**, 1-15.

Sun, H. and Faltinsen, O.M. (2006), "Water impact of horizontal circular cylinders and cylindrical shells", *Appl. Ocean Res.*, **28**, 299-311.

Sun, Z., Xing, J.T., Djidjeli, K. and Cheng, F. (2015), "Coupling MPS and modal superposition method for flexible wedge dropping simulation", *Proceedings of the 25th International Ocean and Polar Engineering Conference Kona*, Big Island, Hawaii, USA.

Tay, Z.Y. and Wang, C.M. (2012), "Reducing hydroelastic response of very large floating structures by altering their plan shapes", *Ocean Syst. Eng.*, **2**(1), 69-81.

Tsuruta, N., Khayyer, A. and Gotoh, H. (2013), "A short note on dynamic stabilization of moving particle semi-implicit method", *Comput. Fluids*, **82**, 158-164.

Tsuruta, N., Khayyer, A. and Gotoh, H. (2016), "A novel refinement technique for projection-based particle methods", *Proceedings of the 11th international SPHERIC workshop*, Munich, Germany, June 2016.

Wagner, H. (1932), "Über stoss und gleitvorgänge an der oberfläche von flüssigkeiten", Zeitschrift für Angewandte Mathematik und Mechanik, **12**.

Wang, J., Lugni, C. and Faltinsen, O.M. (2015), "Experimental and numerical investigation of a freefall wedge vertically entering the water surface", *Appl. Ocean Res.*, **51**, 181-203.

Wendland, H. (1995), "Piecewise polynomial, positive definite and compactly supported radial functions of minimal degree", *Adv. Comput. Math.*, **4**, 389-396.

Yang, Q., Jones, V. and McCue, L. (2012), "Free-surface flow interactions with deformable structures using an SPH–FEM model", *Ocean Eng.*, **55**, 136-147.

Zhang, Y., Tang, Z. and Wan, D. (2016), "MPS-FEM coupled method for interaction between sloshing flow and elastic structure in rolling tanks", *Proceedings of the 7th International Conference on Computational Methods (ICCM2016)*, August 1st-4th, Berkeley, CA, USA.

Zhao, R. and Faltinsen, O.M. (1993), "Water entry of two-dimensional bodies", *J. Fluid Mech*., **246**, 593-612.
Zhao, Y., Chen, H.C. and Yu, X. (2015), "Numerical simulation of wave slamming on 3D offshore platform deck using a coupled Level-Set and Volume-of-Fluid method for overset grid system", *Ocean Syst. Eng.*, **5**(4), 245-259.

MK